

Supplement of Atmos. Chem. Phys., 17, 10879–10892, 2017  
<https://doi.org/10.5194/acp-17-10879-2017-supplement>  
© Author(s) 2017. This work is distributed under  
the Creative Commons Attribution 3.0 License.



*Supplement of*

## **Contributions of transported Prudhoe Bay oil field emissions to the aerosol population in Utqiagvik, Alaska**

**Matthew J. Gunsch et al.**

*Correspondence to:* Kerri A. Pratt ([prattka@umich.edu](mailto:prattka@umich.edu))

The copyright of individual parts of the supplement might differ from the CC BY 3.0 License.

## Particle Type Classification

SSA was characterized by an intense peak at  $m/z$  23, corresponding to  $\text{Na}^+$ , and less intense peaks at  $m/z$  39 ( $\text{K}^+$ ), 81 ( $\text{Na}_2\text{Cl}^+$ ), -35,37 ( $\text{Cl}^-$ ) and -93,95 ( $\text{NaCl}_2^-$ ) (Ault et al., 2013). Mass spectra that also contained intense markers for nitrate ( $m/z$  -46, -62) or sulfate ( $m/z$  -64, -80) were sub-classified as aged SSA. Organic carbon (OC) particles were characterized by intense peaks at  $m/z$  37 ( $\text{C}_3\text{H}^+$ ) and 27 ( $\text{C}_2\text{H}_3^+$ ) and are attributed to combustion (Toner et al., 2008). OC particles also contained minor contributions from  $m/z$  12 ( $\text{C}^+$ ), identified as a potential OC fragment by Silva and Prather (2000). A sub-classification of OC particles was characterized by an intense peak at  $m/z$  59 ( $\text{N}(\text{CH}_3)_3^+$ ), which is characteristic of the presence of trimethylamine (TMA) (Rehbein et al., 2011) and has been detected previously in the Arctic (Willis et al., 2016). Rehbein et al. (2011) found that TMA was exclusively found during high relative humidity or fog events when gas phase TMA partitioned onto the particles or fog droplets. Relative humidity was high throughout the duration of the study (average of 91%), thus partitioning of TMA to the particle-phase is likely to occur. Due to the small number of TMA-containing particles measured, both OC particle types were grouped into a single OC class. Soot particles were characterized by elemental carbon  $\text{C}_n^+$  fragment peaks, observed at  $m/z$  12 ( $\text{C}^+$ ), 24 ( $\text{C}_2^+$ ), 36 ( $\text{C}_3^+$ ), 48 ( $\text{C}_4^+$ ), etc., that are typical of incomplete combustion (Toner et al., 2008). Biomass burning (BB) particles were characterized by an intense peak at  $m/z$  39 ( $\text{K}^+$ ) and  $m/z$  -97 ( $\text{HSO}_4^-$ ) with less intense peaks at  $m/z$  43 ( $\text{C}_3\text{H}_2\text{O}^+$ ), 27 ( $\text{C}_2\text{H}_3^+$ ) and 12 ( $\text{C}^+$ ) (Pratt et al., 2011). Dust was present in two different forms: calcium-rich and iron-rich. Calcium-rich dust (Ca-Dust) was characterized by an intense peak at  $m/z$  40 ( $\text{Ca}^+$ ) with less intense peaks at  $m/z$  23 ( $\text{Na}^+$ ), 24 ( $\text{Mg}^+$ ) and 56,57 ( $\text{CaOH}^+$ ,  $\text{CaOH}_2^+$ ). Iron-rich dust (Fe-dust) was characterized by intense peaks at  $m/z$  54,56 ( $\text{Fe}^+$ ). All dust particle types were combined into a single cluster, as the majority likely originated from the nearby beaches, dirt roads and soil. Average spectra for each particle type are shown in Figure 4.

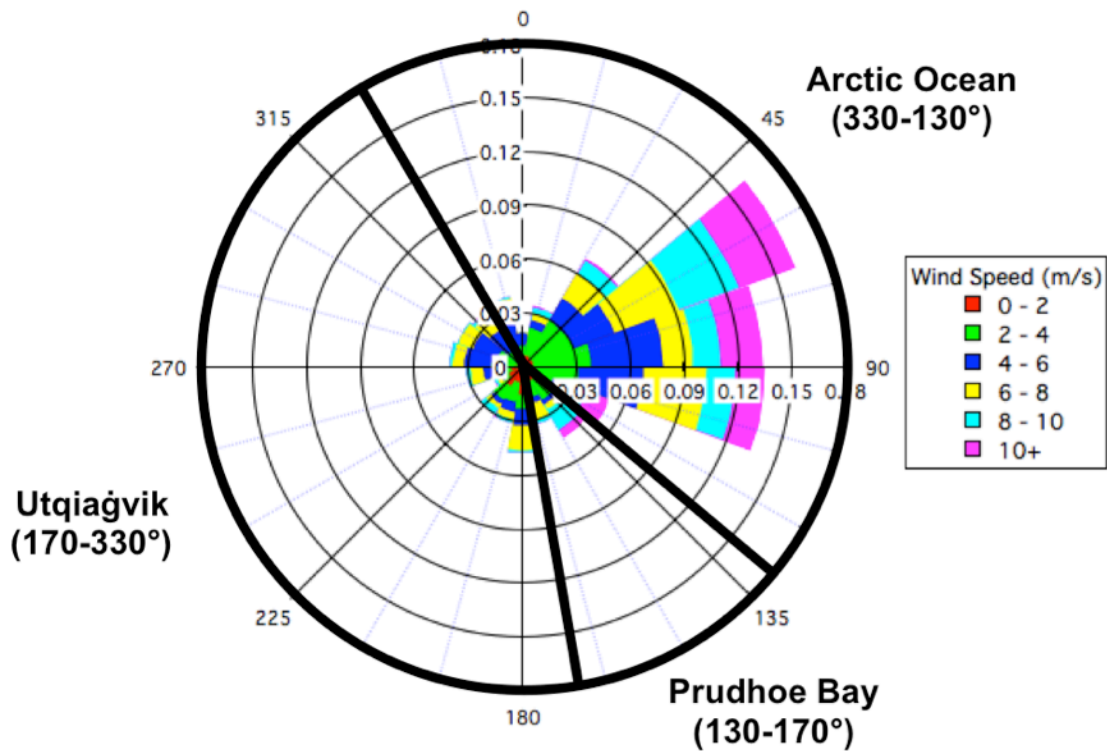
Particle types were identified based on observed morphology from SEM as well as composition and atomic percentages calculated from the EDX spectra. These classes are based on prior SEM-EDX studies, which established EDX spectra for fresh and aged SSA (Ault et al., 2013; Hara et al., 2003),

organic carbon aerosol (Laskin et al., 2006; Moffet et al., 2010), soot (Jiang et al., 2011), biomass burning aerosol (Li et al., 2003; Pósfai et al., 2003), and mineral dust (Coz et al., 2009; Sobanska et al., 2003). Fresh SSA was characterized by large amounts Na and Cl, with Na/Mg and Na/Cl ratios close to those found in seawater. Aged SSA was characterized by Na and S and/or N > Cl, indicative of chlorine displacement by heterogeneous reactions (Laskin et al., 2003; Laskin et al., 2002). OC particles were round and contained large amounts of C and O with the majority also containing small fractions of S and/or N (Moffet et al., 2010). Soot was primarily carbon in composition and had a chain-like agglomerate morphology (Quennehen et al., 2012; Weinbruch et al., 2012). Dust particles were characterized by large fractions of Al and Si, in addition to trace metals such as Fe (Coz et al., 2009; Sobanska et al., 2003). Some fly ash particles, primarily aluminum and silicon oxides, may also be present in this class, but due to similarities in chemical composition between fly ash and dust accompanied by low abundance, fly ash and dust will be considered together. Minor contributions from BB were also identified, characterized by large amounts of K and Cl but little Na (Pósfai et al., 2003). A sulfur-rich particle type was identified by greater amounts of S as compared to C and O. This is likely the “missing” particle type unable to be characterized by the ATOFMS in this study, as well as the previous ATOFMS study by Sierau et al. (2014). Wenzel et al. (2003) previously attributed scattered, but not ionized particles by ATOFMS, as relatively pure ammonium sulfate particles.

## References

- 45 Ault, A.P., Guasco, T.L., Ryder, O.S., Baltrusaitis, J., Cuadra-Rodriguez, L.A., Collins, D.B., Ruppel, M.J., Bertram, T.H., Prather, K.A., Grassian, V.H., 2013. Inside versus outside: Ion redistribution in nitric acid reacted sea spray aerosol particles as determined by single particle analysis. *J. Am. Chem. Soc.* 135, 14528-14531.
- 50 Coz, E., Gómez-Moreno, F.J., Pujadas, M., Casuccio, G.S., Lersch, T.L., Artíñano, B., 2009. Individual particle characteristics of North African dust under different long-range transport scenarios. *Atmos. Environ.* 43, 1850-1863.
- Hara, K., Yamagata, S., Yamanouchi, T., Sato, K., Herber, A., Iwasaka, Y., Nagatani, M., Nakata, H., 2003. Mixing states of individual aerosol particles in spring Arctic troposphere during ASTAR 2000 campaign. *J. Geophys. Res-Atmos.* 108.
- 55 Jiang, M.Y., Li, J.Q., Wu, Y.Q., Lin, N.T., Wang, X.M., Fu, F.F., 2011. Chemical characterization of nanometer-sized elemental carbon particles emitted from diesel vehicles. *J. Aerosol. Sci.* 42, 365-371.
- Laskin, A., Cowin, J.P., Iedema, M.J., 2006. Analysis of individual environmental particles using modern methods of electron microscopy and X-ray microanalysis. *J. Electron. Spectrosc.* 150, 260-274.
- 60 Laskin, A., Gaspar, D.J., Wang, W., Hunt, S.W., Cowin, J.P., Colson, S.D., Finlayson-Pitts, B.J., 2003. Reactions at interfaces as a source of sulfate formation in sea-salt particles. *Science* 301, 340-344.
- Laskin, A., Iedema, M.J., Cowin, J.P., 2002. Quantitative time-resolved monitoring of nitrate formation in sea salt particles using a CCSEM/EDX single particle analysis. *Environ. Sci. Technol.* 36, 4948-4955.
- 65 Li, J., Pósfai, M., Hobbs, P.V., Buseck, P.R., 2003. Individual aerosol particles from biomass burning in southern Africa: 2, Compositions and aging of inorganic particles. *J. Geophys. Res-Atmos.* 108.
- Moffet, R.C., Henn, T., Laskin, A., Gilles, M.K., 2010. Automated Chemical Analysis of Internally Mixed Aerosol Particles Using X-ray Spectromicroscopy at the Carbon K-Edge†. *Anal. Chem.* 82, 7906-7914.
- 70 Pósfai, M., Simonics, R., Li, J., Hobbs, P.V., Buseck, P.R., 2003. Individual aerosol particles from biomass burning in southern Africa: 1. Compositions and size distributions of carbonaceous particles. *J. Geophys. Res-Atmos.* 108.
- 75 Pratt, K., Murphy, S., Subramanian, R., DeMott, P., Kok, G., Campos, T., Rogers, D., Prenni, A., Heymsfield, A., Seinfeld, J., 2011. Flight-based chemical characterization of biomass burning aerosols within two prescribed burn smoke plumes. *Atmos. Chem. Phys.* 11, 12549-12565.
- 80 Quennehen, B., Schwarzenboeck, A., Matsuki, A., Burkhardt, J., Stohl, A., Ancellet, G., Law, K.S., 2012. Anthropogenic and forest fire pollution aerosol transported to the Arctic: observations from the POLARCAT-France spring campaign. *Atmos. Chem. Phys.* 12, 6437-6454.
- Rehbein, P.J., Jeong, C.-H., McGuire, M.L., Yao, X., Corbin, J.C., Evans, G.J., 2011. Cloud and fog processing enhanced gas-to-particle partitioning of trimethylamine. *Environ. Sci. Technol.* 45, 4346-4352.

- 85 Sierau, B., Chang, R.-W., Leck, C., Paatero, J., Lohmann, U., 2014. Single-particle characterization of the high-Arctic summertime aerosol. *Atmos. Chem. Phys.* 14, 7409-7430.
- Silva, P.J., Prather, K.A., 2000. Interpretation of mass spectra from organic compounds in aerosol time-of-flight mass spectrometry. *Anal. Chem.* 72, 3553-3562.
- Sobanska, S., Coeur, C., Maenhaut, W., Adams, F., 2003. SEM-EDX characterisation of tropospheric aerosols in the Negev desert (Israel). *J. Atmos. Chem.* 44, 299-322.
- 90 Toner, S.M., Shields, L.G., Sodeman, D.A., Prather, K.A., 2008. Using mass spectral source signatures to apportion exhaust particles from gasoline and diesel powered vehicles in a freeway study using UF-ATOFMS. *Atmos. Environ.* 42, 568-581.
- Weinbruch, S., Wiesemann, D., Ebert, M., Schütze, K., Kallenborn, R., Ström, J., 2012. Chemical composition and sources of aerosol particles at Zeppelin Mountain (Ny Ålesund, Svalbard): An electron microscopy study. *Atmos. Environ.* 49, 142-150.
- 95 Wenzel, R.J., Liu, D.Y., Edgerton, E.S., Prather, K.A., 2003. Aerosol time - of - flight mass spectrometry during the Atlanta Supersite Experiment: 2. Scaling procedures. *J. Geophys. Res-Atmos.* 108.
- 100 Willis, M.D., Burkart, J., Thomas, J.L., Köllner, F., Schneider, J., Bozem, H., Hoor, P.M., Aliabadi, A.A., Schulz, H., Herber, A.B., 2016. Growth of nucleation mode particles in the summertime Arctic: a case study. *Atmos. Chem. Phys.* 15, 7663-7679.



105 **Figure S1.** Wind rose from August 21–September 30, 2015 measured at the NOAA Barrow Observatory. Wind speed is binned by 2 m/s, and wind direction is binned by 20 degrees, with the radial axes representing the fraction of the study under those wind conditions.

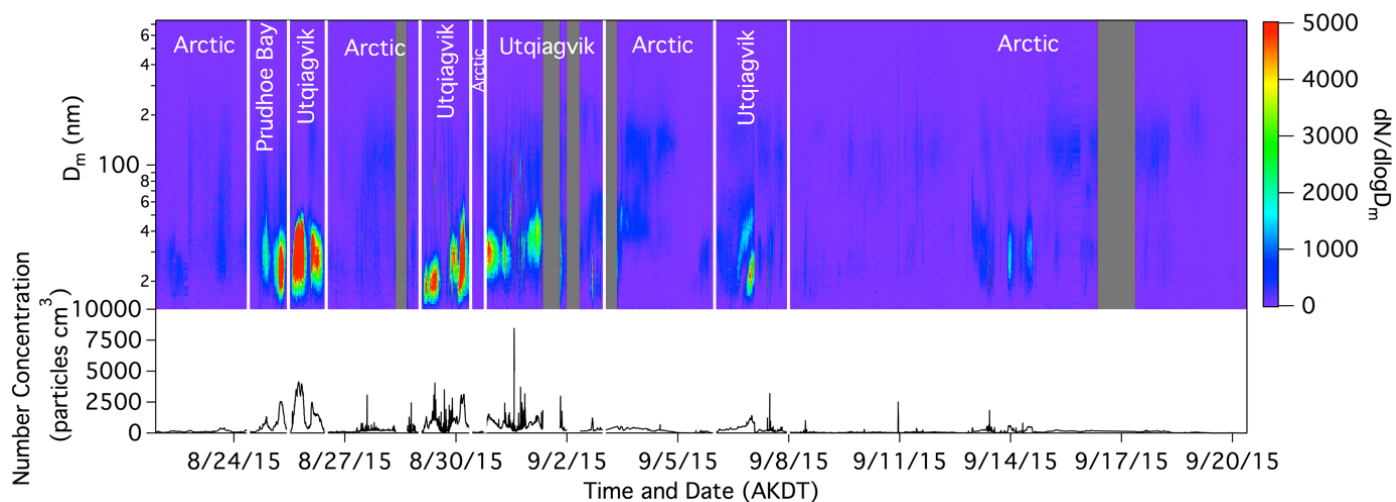
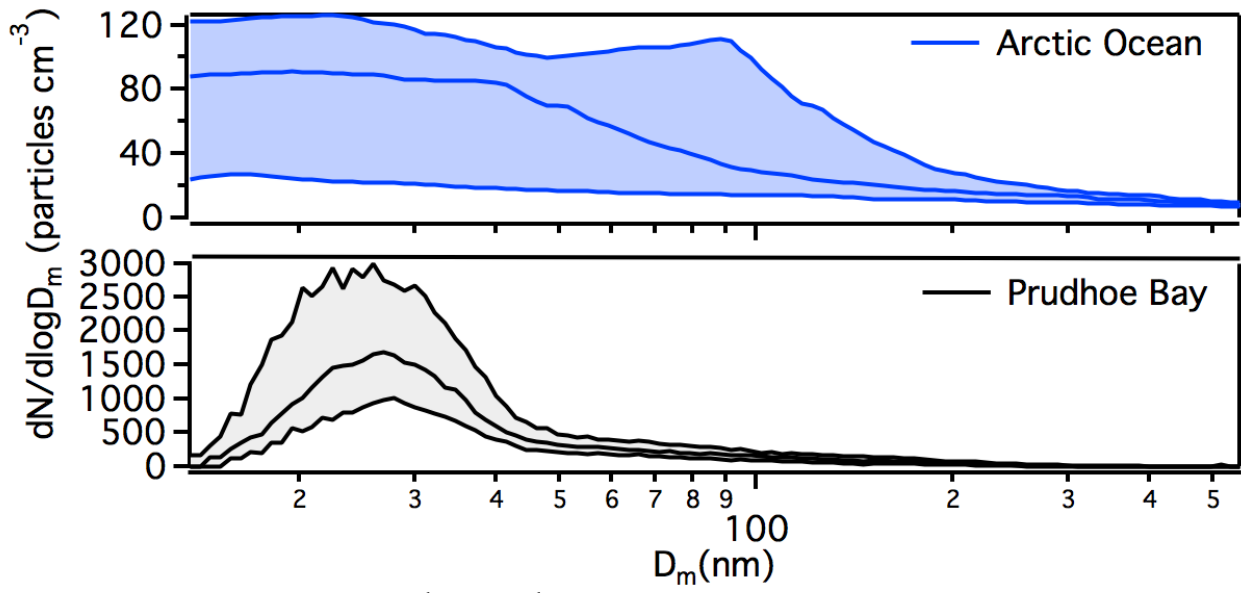


**Figure S2.** Aerosol size-resolved number concentrations (mobility diameter) measured by the SMPS from August 21-September 20, 2015. Identified air mass source regions, determined based on wind direction and backward air mass trajectories, are labeled and divided by white lines in the time series. 115 Periods lacking data are indicated in gray. Total particle (0.013 – 746 nm) number concentrations are also shown.



120 **Figure S3.** Median, as well as 25<sup>th</sup> and 75<sup>th</sup> percentile, particle size distributions, measured by SMPS, during Prudhoe Bay and Arctic Ocean influenced air masses from August 21–September 20, 2015.

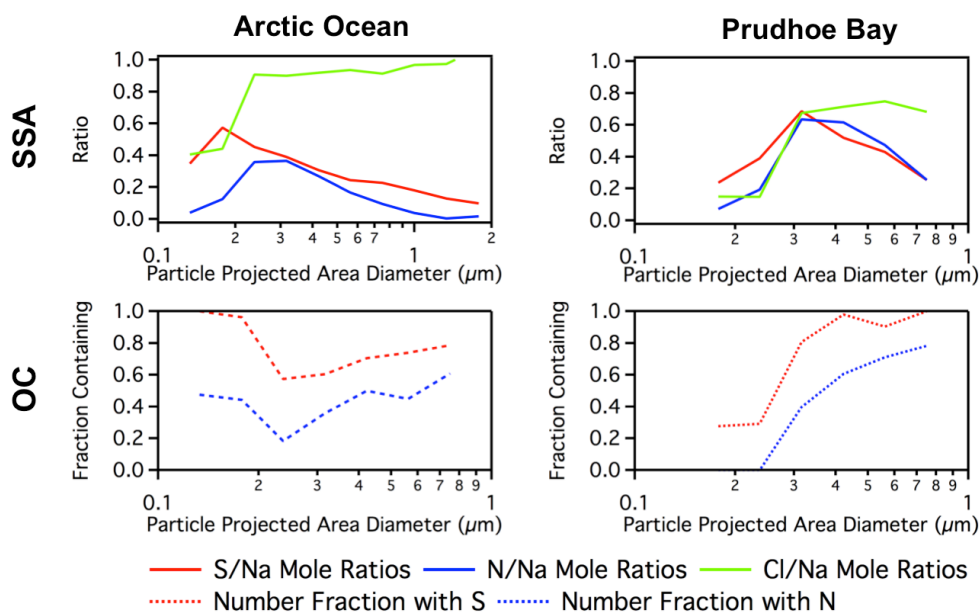


**Figure S4.** S/Na, N/Na, Cl/Na mole ratios of individual SSA (top) and fraction of OC particles (bottom) containing S, N, and/or Cl, measured by CCSEM-EDX for Arctic Ocean and Prudhoe Bay influenced air masses. Size bins with less than 25 particles are not displayed.

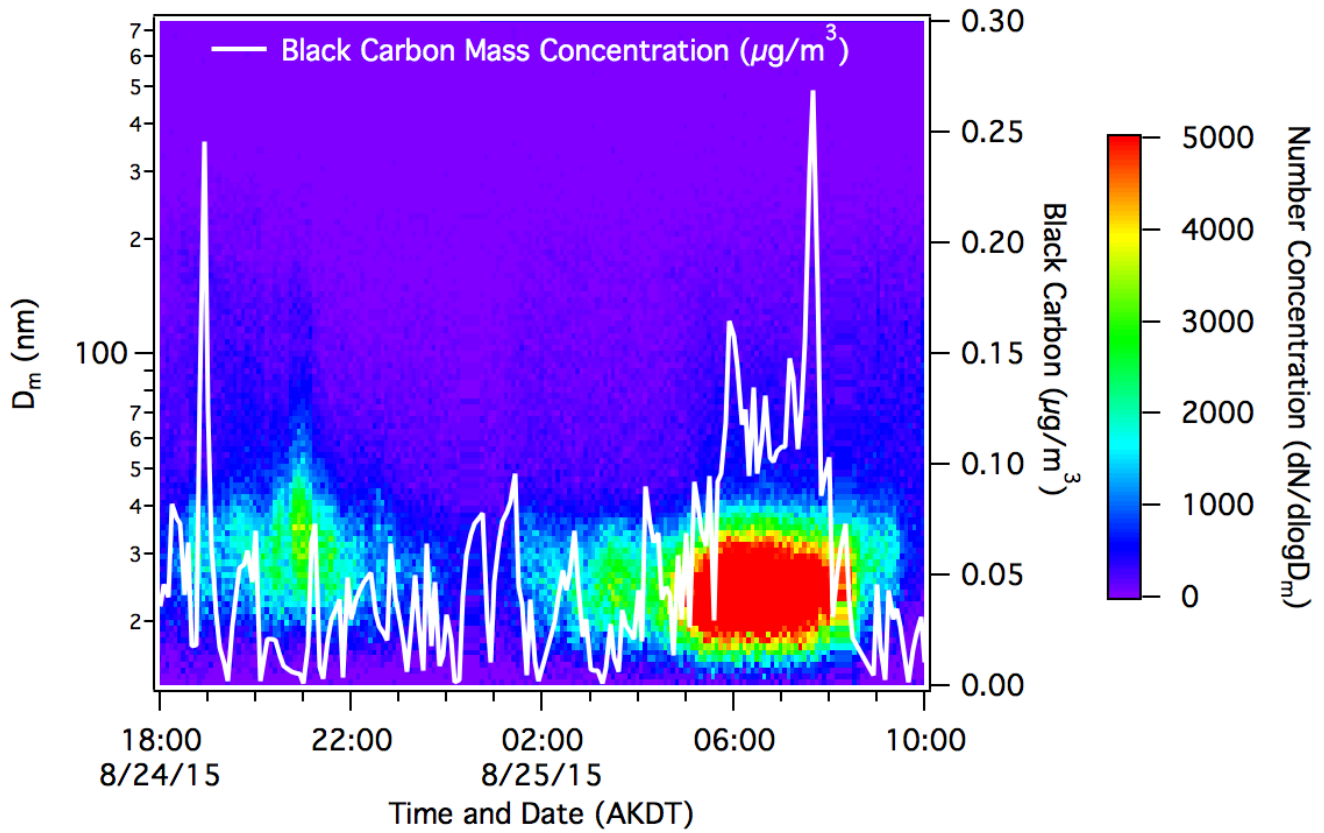


**Figure S5.** Aerosol size-resolved number concentrations (mobility diameter) measured by the SMPS during Prudhoe Bay air mass influence on August 24-25, 2015. Black carbon mass concentrations measured by the aethalometer are overlaid in white.

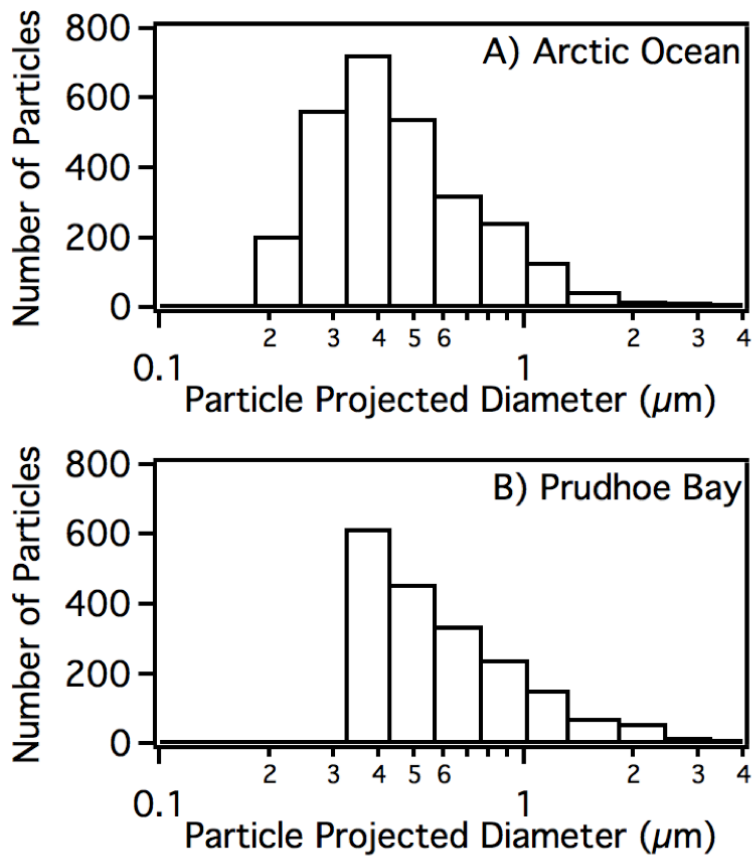


**Figure S6.** Numbers of particles, per particle projected diameter size bin, analyzed by CCSEM-EDX for (A) Arctic Ocean and (B) Prudhoe Bay air mass samples.